Mon. Not. R. astr. Soc. (1969) **144**, 425–448.

DYNAMICS OF SELF-GRAVITATING GASEOUS SPHERES—III

Analytical Results in the Free-fall of Isothermal Cases

M. V. Penston

(Received 1969 March 5)

SUMMARY

For a cold gas, the analytical solutions for collapse in various symmetries give density and velocity profiles at the instant when a singularity develops in the initially densest part. These profiles follow generally from assuming that the density variation is smooth initially. For spherical and planar symmetries we have extended these solutions to a short time before this singularity occurs.

The spherical results are given in Sections 2–4 and imply a density law proportional to $r^{-12/7}$. The planar results follow in Appendix I and the cylindrical ones in Appendix II. The solutions before the singularity arises are similarity solutions with the density and velocity profiles retaining their shapes while altering only their scales with time.

Applying these results we find a spherical collapse to form a galaxy is modified by the rise in central optical depth at a density of $\sim 10^{-20}$ g cm^{-3}. Flattening instabilities are resisted but not overcome by the more rapid growth of the density gradient which occurs in a planar collapse.

In Section 5, a similarity solution for the spherical collapse of an isothermal gas is presented. This has a critical point similar to those found in solar wind flows. The density profile when the singularity arises is proportional to r^{-2}. The collapse of a proto-star is halted by the rise in optical depth when the density reaches 10^{-18} g cm^{-3}. The stability of this solution and the problem of whether all flows converge to it still remain to be settled.

1. INTRODUCTION

It seems probable that both stars and galaxies form from larger accumulations of matter collapsing under their own self-gravitational attraction. Although the instabilities that lead to this collapse are fairly well understood, the detailed behaviour of the collapse stages has not been thoroughly explored. In the case of star-formation the final stage, that of pre-main-sequence evolution, is consequently lacking suitable initial conditions. Moreover it is quite likely that some infra-red stars are undergoing the pre-stellar collapse phase, so that an understanding of such objects awaits a complete description of the formation process. On the other hand, in the case of galaxy formation, one might inquire to what extent the present observed features of galaxies are derived from the details of the collapse phase.

To study the self-gravitational collapse of stars and galaxies we must solve the equations of hydrodynamics including the effects of self-gravitation. Other papers in this series (Penston 1966; Penston 1969a—hereinafter referred to as Papers I and II respectively) report on numerical integrations of these equations. The present paper on the other hand presents analytical solutions for the cases where the gas is either free-falling or isothermal.

There are several motives for trying to find analytical solutions to this problem. Although analytical methods cannot rival the general scope of numerical methods, which can compare the effects of different cooling laws or equations of state with great ease, an analytical solution will be immediately helpful in checking numerical work. Moreover analytical solutions will display the essence of the problem in a much clearer way than numerical ones and enable conclusions to be reached with greater certainty. Finally the analytical solutions given may have uses as initial conditions for later stages of star and galaxy formation or as zero-order solutions which may be perturbed to study such topics as fragmentation.

The results of Paper II show that the free-fall and isothermal cases are particularly interesting. When galaxies form the final collapse takes place essentially in free-fall since the cooling mechanisms of the ionized intergalactic medium, which are two-particle processes such as recombination radiation, overwhelm the heating mechanisms such as cosmic ray heating (one-particle) in condensations, and bring the temperature down to about 5000 °K, much too cool to support a proto-galaxy. On the other hand in the case of star-formation approximate isothermality is retained at about 10 °K due to the extreme temperature-sensitivity of the cooling-rate due to electron collisions with C^+, and this temperature is high enough that pressure forces affect the collapse.

In Paper II we define certain dimensionless ratios by which self-gravitating flows can be classified. For convenience we redefine them now:

The Jeans number $$J = \frac{\text{gravitational energy}}{\text{thermal energy}},$$

Dimensionless cooling time $$\tau_c = \frac{\text{cooling (or heating) time}}{\text{sound-travel time}},$$

(Effective) ratio of specific heats $$\gamma = \frac{\partial(\log P)}{\partial(\log \rho)}.$$

Thus the free-fall case is clearly described by $J \gg 1$, while the isothermal solution will have $J \gtrsim 1$, $\tau_c \gg 1$ and $\gamma = 1$.

Solutions with these values of J, τ_c and γ have already been integrated numerically. An example of the free-fall case is model GIII of Paper II and of the isothermal case is case (iv) of Paper I. Now it is commented in Paper II that density profiles near the centre show the forms $\rho \propto r^{-12/7}$ in the free-fall and $\rho \propto r^{-2}$ in the isothermal cases. Bodenheimer & Sweigert (1968) were the first to draw attention to the isothermal result. Fig. 1 displays these profiles, which plainly suggest that asymptotic similarity solutions exist. It is these similarity solutions that are derived here.

It should be stressed that the solutions given here are of a different character to those obtained by others. The 'linear-wave' solutions of McVittie (1956) and Disney, McNally & Wright (1968) suffer the disadvantage that the cooling rate of the gas in the collapsing sphere is imposed by the solution rather than by any physical considerations. Neither do they display the property of a rapid enhancement of the central density found in most numerical computations. It is well-known that the problem of cold freely-falling gas can be solved with various assumptions about the symmetry (e.g. Mestel 1965) but these solutions have not before been displayed in the forms given here and in the appendices which make their similarity properties evident.

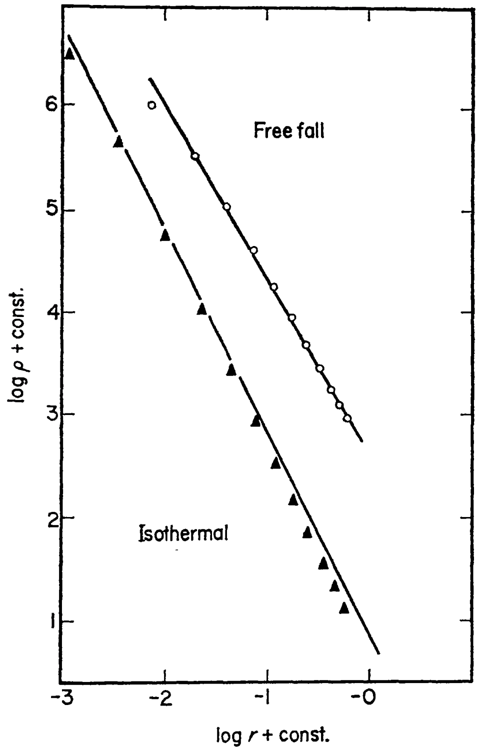

FIG. 1. *Results of numerical calculations displaying the existence of similarity solutions. The circles are taken from the density–radius relation found numerically in the freely falling model GIII of Paper II and the straight line through them has slope* $-12/7$. *The triangles are similarly from a numerical solution of isothermal collapse—case* (*iv*) *of Paper I—and the straight line has slope* -2.

It is to be regretted that the solutions given here must assume strict spherical symmetry in order to make progress. This means that such potentially important effects as magnetism, rotation and fragmentation must be neglected for the present discussion. However the existence of solutions with other symmetries in the free-fall case given in appendices enables us to make some remarks about flattening instabilities (Lynden-Bell 1964; Mestel 1965), and as commented above the flows presented here could be used as zero-order solutions onto which perturbations could be introduced to study fragmentation.

2. THE FINAL STATE OF A FREE-FALL COLLAPSE

As discussed above the final stages of the collapse of a galaxy are carried out in free-fall. We consider a sphere of gas initially at rest and with a density $\bar{\rho}(a)$ as the mean density inside radius a and M_a as the total mass inside radius a. We further take the sphere of gas to be sufficiently cold that the pressure may be neglected, returning to consider any breakdown of this assumption later.
i.e.

$$M_a = \frac{4\pi}{3} a^3 \bar{\rho}(a) = \int_0^a 4\pi x^2 \rho(x)\, dx.$$

The equation of motion for this system is:

$$\frac{d^2r}{dt^2} = \frac{dv}{dt} = -\frac{GM_a}{r^2} \tag{1}$$

where r and v are distance from the centre and velocity at time t of material initially at a and G is the gravitational constant. The parametric solution of this equation is (Mestel 1965)

$$\left.\begin{aligned} r &= a\cos^2\theta \\ t &= \left\{\frac{8\pi}{3}G\bar{\rho}(a)\right\}^{-1/2}(\theta+\tfrac{1}{2}\sin 2\theta) \end{aligned}\right\} \qquad (2)$$

where θ is the parameter. Note that for a small $r \to 0$ when:

$$t = t_f = \left(\frac{3\pi}{32G\rho_0}\right)^{1/2}$$

where

$$\rho_0 = \bar{\rho}(0) = \rho(0).$$

Now let us assume that ρ has a smooth maximum at the centre so that $\bar{\rho}(a)$ also has a smooth maximum there at $a = 0$; in Section 4 we shall consider briefly the case where this is not so. Then if the distribution of density is to be free of discontinuities at $t = 0$ and all later times we are able to write:

$$\bar{\rho}(a) = \rho_0\left(1-\frac{a^2}{A^2}\right)$$

for sufficiently small a, where A is a constant.

Note that there is no first order term in a in our expansion for $\bar{\rho}(a)$. Such a term would imply a discontinuity in the pressure gradient which would generate discontinuities in velocity and density in turn. In exceptional cases, the coefficient of a^2 in the expansion of $\bar{\rho}(a)$ is zero when the solution we obtain below will no longer apply. However we are ' almost always ' correct in taking the form of $\bar{\rho}(a)$ given above.

At time $t = t_f$, the value of $\theta(a)$—that value of θ appropriate for material initially at distance a from the centre—is given by:

$$\left(\frac{3\pi}{32G\rho_0}\right)^{1/2} = \left(\frac{3}{8\pi G\bar{\rho}(a)}\right)^{1/2}(\theta(a)+\tfrac{1}{2}\sin 2\theta(a)).$$

Express $\theta(a) = (\pi/2)-\chi(a)$ and note is a is sufficiently small $\chi(a) \ll (\pi/2)$, so that:

$$1 = \left(1+\frac{1}{2}\frac{a^2}{A^2}\right)\left(1-\frac{4}{3\pi}\chi^3(a)\right)$$

i.e.

$$\chi^3(a) = \frac{3\pi}{8}\frac{a^2}{A^2}.$$

Now we note that:

$$r = a\chi^2 = a\left(\frac{3\pi}{8}\frac{a^2}{A^2}\right)^{2/3} \propto a^{7/3}.$$

It is now a straightforward matter to obtain the density distribution in the sphere at the moment at which the singularity arises in the centre, for we have

$$\rho \sim \rho_0\frac{a^2}{r^2}\frac{da}{dr} \propto \frac{r^{6/7}}{r^2}r^{-4/7} = r^{-12/7}. \qquad (3)$$

This is precisely the result found from the numerical integrations of model GIII of Paper II. Moreover we have shown that this profile arises inevitably near the centre assuming only that the mean density $\bar{\rho}$ has a smooth maximum at the centre. In practise one might reasonably expect the collapse to be centred about the densest regions—thus it follows that this density profile is of general significance. We may also obtain the velocity distribution since we have an integral of the equation of motion (1):

$$\frac{1}{2}v^2 - \frac{GM_a}{r} = \text{constant.}$$

Now whatever the initial value of the constant, for small enough a, we find as $r \to 0$ at the centre that:

$$v = -\sqrt{\frac{2GM_a}{r}} \propto -\left(\frac{r^{9/7}}{r}\right)^{1/2} = -r^{1/7}. \qquad (4)$$

We have already commented that the free-fall case has a Jeans number very large, let us now consider the ratio of gravitational and pressure *forces*:

$$J^* = \frac{\text{gravitational forces}}{\text{thermal forces}} = \frac{\dfrac{GM_a}{r^2}}{\dfrac{1}{\rho}\dfrac{d}{dr}\dfrac{\mathcal{R}T}{\mu}\rho}$$

where T is the temperature, $\mathcal{R}$ the gas constant and μ the mean molecular weight. If the variations of T near the centre are small at $t = t_f$

$$J^* \propto \frac{r^{-5/7}}{r^{-1}} = r^{2/7}.$$

In other words pressure must be important at the centre however large the Jeans number and our solution breaks down there. This result confirms analytically the discussion in Paper II which showed that $J \gg 1$ implies that pressure forces, while unimportant in the flow at large, remain important in certain singular regions.

When projected on the sky, a spherical distribution of matter is seen as a circular distribution of surface density obtained by integrating the true density along each line of sight (see Penston 1969b). We shall term this surface density the ' projected surface density ' of the original sphere. Let $\sigma(R)$ be the projected surface density of our gas sphere viewed at a projected distance R from the centre.

Then

$$\sigma(R) = 2\int_R^\infty \frac{\rho(r)\, r dr}{\sqrt{(r^2 - R^2)}}.$$

If $\rho \propto r^{-12/7}$ we find $\sigma \propto R^{-5/7}$ so that the projected surface density of the centre is infinite. This shows that the optical depth of the central regions of the sphere at $t = t_f$ will be large. They will then be thermally isolated from their surroundings and will behave adiabatically. The resultant compressional heating may also cause deviations from the solution in equation (3).

Thus we expect the collapse of a galaxy, proceeding in free-fall, to develop a runaway singularity at the initially densest part of the flow, and that the density profile should approach an $r^{-12/7}$ law near the centre. However this process will be halted at the centre by the re-emergence of the importance of the thermal energy in a small region near the centre either due to the high density gradient or the increase of optical depth and accompanying compressional heating.

3. THE ASYMPTOTIC SOLUTION IN THE FREE-FALL CASE

It turns out that we can examine the onset of these effects analytically. In Section 2 we made an expansion in space to small distances from the centre at the moment the singularity actually appeared. Now we extend this to a time $t = t_f - \delta t$ just before the singularity arises so that we can determine whether the rise in density gradient or increase in optical depth first slows the collapse of a galaxy. We relate $\chi(a)$ and δt by equation (2) to obtain:

$$\frac{t}{t_f} = 1 - \frac{\delta t}{t_f} = \left(1 + \frac{1}{2}\frac{a^2}{A^2}\right)\left(1 - \frac{4}{3\pi}\chi^3(a)\right)$$

whence

$$\chi^3(a) = \frac{3\pi}{4}\left\{\frac{\delta t}{t_f} + \frac{1}{2}\frac{a^2}{A^2}\right\}.$$

Again from equation (2) we see that

$$r = a\left\{\frac{3\pi}{4}\left(\frac{\delta t}{t_f} + \frac{1}{2}\frac{a^2}{A^2}\right)\right\}^{2/3} \tag{5}$$

and hence

$$\frac{dr^3}{da} = \left(\frac{3\pi}{4}\right)^2\left(3a^2\left(\frac{\delta t}{t_f}\right)^2 + 10a^4\left(\frac{1}{2A^2}\right)\left(\frac{\delta t}{t_f}\right) + 7a^6\left(\frac{1}{2A^2}\right)^2\right),$$

which gives the density profile

$$\rho = \left(\frac{3\pi}{4}\right)^{-2} \frac{3\rho_0}{3\left(\frac{\delta t}{t_f}\right)^2 + 10\left(\frac{a^2}{2A^2}\right)\left(\frac{\delta t}{t_f}\right) + 7\left(\frac{a^2}{2A^2}\right)^2}.$$

So that when we define the central density

$$\rho_c = \left(\frac{3\pi}{4}\right)^{-2}\rho_0\left(\frac{t_f}{\delta t}\right)^2$$

and

$$\beta = \left(\frac{a^2}{2A^2}\right)\left(\frac{t_f}{\delta t}\right).$$

We find that

$$\frac{\rho}{\rho_c} = \frac{3}{3 + 10\beta + 7\beta^2}. \tag{6}$$

We see we may rewrite equation (5) as

$$\frac{r}{r_0} = \sqrt{\beta}(1+\beta)^{2/3} \tag{7}$$

where r_0 is the time-dependent length scale

$$r_0 = \left(\frac{3\pi}{4}\right)^{2/3}\sqrt{2}\,A\left(\frac{\delta t}{t_f}\right)^{7/6}.$$

We have found the density profile in the form of equations (6) and (7) and the definitions of ρ_c and r_0 above at time $t_f-\delta t$ just before the singularity occurs. To complete our knowledge of this solution we need the velocity profile.

The integral of equation (1) is

$$v^2 = \frac{2GM_a}{r} = \frac{8\pi}{3} G\rho_0 \frac{a^3}{r}.$$

Into this we substitute for r using equation (7) and use the definition of β and obtain

$$\left(\frac{v}{v_0}\right)^2 = \frac{\beta}{(1+\beta)^{2/3}} \tag{8}$$

where we now define a time dependent velocity scale

$$v_0 = \frac{\pi}{\sqrt{2}} \left(\frac{4}{3\pi}\right)^{1/3} \frac{A}{t_f} \left(\frac{\delta t}{t_f}\right)^{1/6}.$$

Note that β is related to the mass within the shell that it labels. Using the definitions of ρ_c, r_0 and β we can show

$$M_a = \frac{4\pi}{3} \rho_c r_0^3 \beta^{3/2}.$$

Thus equations (6)–(8) give the density and velocity profiles in a parametric form at time $t_f-\delta t$. These profiles are displayed in Fig. 2. We shall discuss some

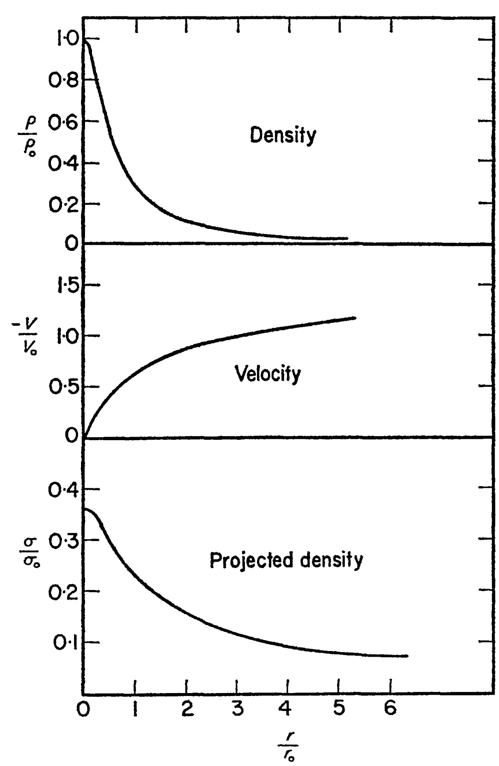

FIG. 2. *The spherical free-fall similarity solution given in equations* (6)–(8) *and Table I. Density, velocity and projected surface density are plotted against radius.*

of their properties. One feature of these solutions is that we may write them in the form:

$$\rho = \rho_c P\left(\frac{r}{r_0}\right), \qquad v = v_0 V\left(\frac{r}{r_0}\right)$$

where all the time dependence is thrown on the quantities ρ_c, v_0 and r_0. The same runs of density and velocity apply at all times and only the scales change. For this reason we recognize these as similarity solutions. They are in fact quite different from other solutions such as the linear-wave flows obtained in the past (McVittie 1956; Disney *et al.* 1968). Our solution retains the generality of that of Section 2—it will occur near the centre wherever a spherical collapse occurs about any density maximum.

Moreover the solution given in equations (6)–(8) can be regarded independently of the approximations by which we have constructed it. In Section 4, we shall show that if the solution is somehow set up over all r at any particular time then it remains true over all r as time passes.

We now relate this similarity solution to the results of Section 2—expanding equations (6)–(8) in the cases $r \ll r_0$ and $r \gg r_0$ respectively:

for $r \ll r_0$:

$$\rho = \rho_c\left(1 - \frac{10}{3}\frac{r^2}{r_0^2}\right)$$

$$\frac{v}{v_0} = -\frac{r}{r_0}$$

and for $r \gg r_0$:

$$\rho = \frac{3}{7}\rho_c\left(\frac{r}{r_0}\right)^{-12/7}$$

$$\frac{v}{v_0} = -\left(\frac{r}{r_0}\right)^{1/7}.$$

Thus we have recovered the results of Section 2 for positions a little away from the centre of the sphere. Moreover if we insert the definitions of ρ_c, r_0 and v_0, we find that the profiles in the regime $r \gg r_0$ are independent of time. This is in accord with expectation since the free-fall time in this region is much greater than δt. Thus our similarity solution shows just the character expected, the outer regions settle down into the $r^{-12/7}$ law while the centre continues its runaway evolution.

We now return to the question of whether the collapse of a galaxy is first affected by the growth of the central density gradient or of the optical depth. We consider these in turn.

The ratio of gravitational to thermal forces may be shown from equations (6)–(8) to have its minimum at the centre of the sphere if the temperature is more or less uniform. There this ratio has the value:

$$J^* = \left|\frac{\dfrac{GM_a}{r^2}}{\dfrac{RT}{\mu}\dfrac{1}{\rho}\dfrac{d\rho}{dr}}\right| = \frac{\pi}{5}\frac{G\rho_c r_0^2}{\mathscr{R}T/\mu}$$

$$= \frac{2\pi}{5}\left(\frac{3\pi}{4}\right)^{-2/3}\frac{G\rho_0 A^2}{\mathscr{R}T/\mu}\left(\frac{\delta t}{t_f}\right)^{1/3}.$$

Galaxies form due to thermal instability. If the proto-galaxy was in equilibrium at a temperature T_i before the collapse and finally settles at a temperature T_f during the collapse, we can write:

$$J^* = \left(\frac{3\pi}{4}\right)^{-2/3} \frac{T_i}{T_f} \left(\frac{\delta t}{t_f}\right)^{1/3}.$$

The temperature of the intergalactic medium is generally thought to be $\sim 3 \times 10^5$ °K, and the temperature of the gas in a collapsing galaxy would probably be $\sim 10^4$ °K about the re-combination temperature of H^+ (see also Paper II) so we deduce that thermal forces become important due to the growth of the density gradient when $J^* = 1$ or

$$\left(\frac{\delta t}{t_f}\right) \sim 10^{-4}.$$

However our lack of firm knowledge about temperature of the intergalactic medium implies that this may be in error by up to a factor of ~ 100. Moreover in Appendix I, we show that our assumption of spherical symmetry is extremely critical in this connection.

If the pressure gradient becomes important due to this cause rather than the rise of optical depth discussed next, we may expect the flow to remain isothermal with the pressure forces remaining important. A similarity solution for such a flow is discussed in Section 5.

Turning to the growth of the optical depth, we first compute the projected surface density profile. As before:

$$\sigma(R) = 2\int_R^\infty \frac{\rho(r)\, r dr}{\sqrt{(r^2 - R^2)}}.$$

Integrating by parts we may rewrite this as:

$$\sigma(R) = -2\int_{R^2}^\infty \sqrt{(r^2 - R^2)}\, \frac{d\rho}{dr^2}\, dr^2.$$

Then substituting equations (6) and (7) we find

$$\sigma(R) = \sigma_0 \int_B^\infty \sqrt{\{\beta(1+\beta)^{4/3} - B(1+B)^{4/3}\}}\, \frac{10+14\beta}{(3+10\beta+7\beta^2)^2}\, d\beta$$

where

$$\frac{R}{r_0} = B^{1/2}(1+B)^{2/3} \text{ and } \sigma_0 = 2\rho_c r_0.$$

It does not appear straightforward to integrate this analytically and therefore it was evaluated for various values of B on a computer. The results of this are shown in Table I and are illustrated in Fig. 2. The profile is much peakier than for example an isothermal gas sphere. Note too that since:

$$\frac{\sigma}{\sigma_0} = \Sigma\left(\frac{R}{r_0}\right)$$

the similarity nature of the solution is evident here.

TABLE I

Projected surface density of asymptotic solution in the free-fall case (see also Fig. 2)

R/r_0	σ/σ_0	R/r_0	σ/σ_0
0·0	0·369	2·121	0·146
0·143	0·360	2·392	0·135
0·205	0·352	2·665	0·126
0·298	0·336	2·942	0·118
0·408	0·298	3·503	0·105
0·595	0·282	3·788	0·100
0·709	0·264	4·075	0·095
0·819	0·248	4·364	0·091
0·900	0·237	4·657	0·087
1·001	0·224	4·951	0·083
1·192	0·206	5·547	0·077
1·403	0·188	6·151	0·071
1·587	0·174	7·072	0·064
1·853	0·159	8·010	0·059

Now using the value of σ/σ_0 at the centre of the sphere we find the central optical depth in the final stages of the collapse τ_f is given by:

$$\tau_f = 0{\cdot}37\,\kappa\sigma_0 = 0{\cdot}74\,\kappa\rho_c r_0$$

where κ is the (single-particle) opacity of the material in the gas sphere. We find:

$$\tau_f = 0{\cdot}74\sqrt{2}\left(\frac{3\pi}{4}\right)^{-4/3}\kappa\rho_0 A\left(\frac{t_f}{\delta t}\right)^{5/6}.$$

Neglecting factors of order ten:

$$\tau_f \sim 0{\cdot}3\,\tau_i\left(\frac{t_f}{\delta t}\right)^{5/6}$$

where τ_i is the initial optical depth of the protogalaxy. A mass of $10^{11}\,M_\odot$ at cosmological densities has an optical depth due to electron scattering ($\kappa = 0{\cdot}3$) of $\tau_i \sim 10^{-5}$. Then the central optical depth rises to 10 when the centre is almost totally thermally isolated when:

$$\frac{\delta t}{t_f} \sim 10^{-4\frac{1}{2}}.$$

Thus the collapse of the centre will be modified by the increase in pressure following the rise of optical depth at this time, by coincidence almost the same as that when the rise in density gradient brings pressure forces into importance. It is interesting to find the density and radius of the runaway nucleus when this happens, we have:

$$\rho_c \sim 10^{-20}\ \mathrm{g\,cm^{-3}}, \qquad r_0 \sim 10^{19\frac{1}{2}}\ \mathrm{cm} \sim 10\ \mathrm{pcs}.$$

So that we have a central condensation of $\sim 10^5\,M_\odot$ formed. Even though pressure forces have risen to oppose the collapse we will not expect an immediate halt to the collapse. The gas has a considerable inward velocity and the rise in importance of radiation pressure will lead to a ratio of specific heats equal to 4/3. The central condensation however eventually must come to equilibrium and continue to accrete material from the rest of the flow.

Away from the centre this infalling gas will still be pressure-free where the optical depth has yet to rise. We can obtain the form of the flow in this region by finding the solution for δt negative, in a parallel way to that where it is positive, now assuming that $|\delta t/t_f| \ll 1$. It turns out that we may extend the solution for δt positive given by equations (6)–(8) writing:

$$\left.\begin{aligned} \frac{\rho}{\rho_c} &= \frac{3}{3+10\beta+7\beta^2} \\ \frac{r}{r_0} &= \sqrt{|\beta|}\,.\,|1+\beta|^{2/3} \\ \left(\frac{v}{v_0}\right)^2 &= \frac{|\beta|}{|1+\beta|^{2/3}} \end{aligned}\right\} \qquad (9)$$

where the time-dependent scales have their definitions extended to accommodate the negative δt.
i.e.

$$\rho_c = \left(\frac{3\pi}{4}\right)^{-2} \rho_0 \left|\frac{t_f}{\delta t}\right|^2$$

$$r_0 = \left(\frac{3\pi}{4}\right)^{2/3} \sqrt{2}\, A \left|\frac{\delta t}{t_f}\right|^{7/6}$$

$$v_0 = \frac{\pi}{\sqrt{2}} \left(\frac{4}{3\pi}\right)^{1/3} \frac{A}{t_f} \left|\frac{\delta t}{t_f}\right|^{1/6}.$$

We see that the branch of the solution for negative δt corresponds to negative β and in particular β running from $-\infty$ to -1. The parts of the sphere far from the centre correspond to β large and negative, while the singularity at the centre corresponds to $\beta = -1$ where there is a point mass of

$$\frac{4\pi}{3} \rho_c r_0^3 = 8\sqrt{\frac{2\pi}{3}}\, \rho_0 A^3 \left|\frac{\delta t}{t_f}\right|^{3/2}.$$

The form of this branch of the solution in the region $r \gg r_0$ is the same as that of Section 2 again but for $r \ll r_0$ we find the relations

$$\frac{\rho}{\rho_c} = \frac{3}{4}\left(\frac{r}{r_0}\right)^{-3/2}, \qquad \frac{v}{v_0} = -\left(\frac{r}{r_0}\right)^{1/2}.$$

However we note that before the centre goes optically thick we are making very drastic assumptions in neglecting any angular momentum or flattening instability and unless the initial conditions are very special, it seems that our approximations will break down. However we show in Appendix I that thermal forces become important due to the rise in density gradient at an earlier stage for free-fall collapse to a plane. So we would expect this to oppose any drastic flattening in the absence of angular momentum.

Nonetheless our similarity solution given by equations (6)–(8) is a general description of spherical collapse in free-fall before a singularity arises in the centre and that given by equations (9) after this time. The similarity solutions retain the essential flavour of the problem in as much as the densest parts run away from the rest of the collapse. It is thus more realistic than previous analytical descriptions of collapse such as uniform spheres and spheroids (explored in detail by Mestel 1965) or linear-wave flows (McVittie 1956; Disney *et al.* 1968).

4. OTHER REMARKS ON THE FREE-FALL CASE

We now return to the assertion made in the last section that the free-fall similarity solution can be derived independently of any approximations. We must show that the flow, given by equations (6)–(8) with the definitions of β and the time-dependent scales, itself satisfies both the equations of motion and continuity for all r. The quantities ρ_0, A and a in these definitions now lose their original meanings although a continues to label shells.

We shall show that the equation of continuity is satisfied if we show that:

$$M_a = \int_0^{r(a,\,t)} 4\pi\rho r^2 dr$$

is independent of time. Substituting for ρ and r from equations (6) and (7) we find:

$$M_a = 4\pi\rho_c r_0^3 \int_0^{\beta(a,\,\delta t)} \frac{3\beta(1+\beta)^{4/3}\{\frac{1}{2}\beta^{-1/2}(1+\beta)^{2/3}+\frac{2}{3}\beta^{1/2}(1+\beta)^{-1/3}\}\,d\beta}{3+10\beta+7\beta^2}.$$

This expression reduces to the simple form:

$$M_a = 4\pi\rho_c r_{0c} \int_0^{\beta(a,\,\delta t)} \tfrac{1}{2}\beta^{1/2}\,d\beta$$

$$= \frac{4\pi}{3}\rho_c r_0^3\,\beta(a,\,\delta t)^{-3/2}.$$

Use of the definitions of ρ_c, r_0 and β show that M_a is indeed independent of time. Thus the solution given in equations (6)–(8) satisfies the continuity equation.

We now show that the solution also satisfies the equation of motion by showing that all shells satisfy its first integral—the energy equation—

$$\frac{GM_a}{r} - \frac{1}{2}v^2 = \text{constant}$$

and that the same constant applies to all shells. We see that

$$\frac{GM_a}{r} = \frac{4\pi}{3}G\rho_c r_0^2 \frac{\beta}{(1+\beta)^{2/3}}$$

and

$$\frac{1}{2}v^2 = \frac{1}{2}v_0^2 \frac{\beta}{(1+\beta)^{2/3}}$$

since use of the definitions of ρ_c, r_0 and v_0 shows that

$$\frac{4\pi}{3}G\rho_c r_0^2 = \frac{1}{2}v_0^2$$

we conclude that

$$\frac{GM_a}{r} - \frac{1}{2}v^2 = 0$$

for all shells and that equation of motion is thus satisfied.

Now we comment briefly on some of the assumptions made in Section 2. We turn first to our assumption that $\bar{\rho}(a)$ is a maximum at the centre. The solution (2) of the equation of motion shows that if $\bar{\rho}(a)$ increases with a, then $r(a) \to 0$ at earlier times for larger a, in other words at some time shells of matter cross and M_a is no longer constant.

To examine this situation more closely we consider the motion of two adjacent shells, initially at a and $a+\Delta a$ and at time t at r and $r+\Delta r$. We have:

$$\frac{d^2r}{dt^2} = -\frac{GM_a}{r^2}$$

$$\frac{d^2}{dt^2}(r+\Delta r) = -\frac{G(M_a+4\pi a^2\,\rho(a)\Delta a)}{(r+\Delta r)^2}$$

i.e. if $\Delta r \ll \Delta a \ll a$

$$\frac{d^2}{dt^2}\Delta r = -2\pi Gm$$

where

$$m = \frac{2a^2\rho(a)\Delta a}{r^2} = 2\rho(r)\Delta r$$

is the mass per unit area contained between $r+\Delta r$ and $r-\Delta r$. We have then the same equation as that governing free-fall collapse in planar symmetry, for which we give a similarity solution in Appendix I.

There are other reasons to believe that the planar case is of some importance. Angular momentum or the Lynden-Bell–Mestel flattening instability (Lynden-Bell 1964; Mestel 1965) both lead to collapse along one axis, so that the results of Appendix I should be quite important.

5. THE SIMILARITY COLLAPSE OF AN ISOTHERMAL SPHERE OF GAS

In earlier chapters we have recovered the $r^{-12/7}$ law found numerically for spheres of gas collapsing in free-fall. We now recall that similar numerical results for isothermal spheres (Bodenheimer & Sweigert 1968, Paper II) gave the different law $\rho \sim r^{-2}$. Now this plainly suggests that a similarity solution of some sort exists. In Paper II we showed that in the final stages of star-formation the collapse is essentially isothermal so that such a solution is likely to be of interest in practice as well as from the theoretical point of view.

The character of the solution found in Section 3 for the free-fall case prompts us to ask if there are any similar solutions for a collapsing isothermal sphere. The equations of motion and continuity in Eulerian co-ordinates, then take the form:

$$\left.\begin{aligned} \frac{\partial v}{\partial t}+v\frac{\partial v}{\partial r} &= -\frac{GM_r}{r^2}-\frac{\mathscr{R}T}{\mu}\frac{\partial}{\partial r}\log\rho \\ \frac{\partial}{\partial t}\log\rho+v\frac{\partial}{\partial r}\log\rho &= -\frac{1}{r^2}\frac{\partial}{\partial r}r^2v \end{aligned}\right\} \qquad (10)$$

where M_r is the mass inside radius r at time t. We add:

$$\frac{\partial M_r}{\partial r} = 4\pi r^2\rho. \qquad (10)$$

We seek similarity solutions of the form:

$$v = v_0 V(x), \qquad \log \rho = \log \rho_0 + Q(x), \qquad M_r = 4\pi \rho_0 r_0^3 N(x)$$

where

$$x = r/r_0$$

and all the time dependence of the system is contained in r_0, v_0 and ρ_0. In the free-fall solutions, we found that the form of these scales came from the initial conditions but here in order to make progress we must use dimensional arguments since the inclusion of the temperature gives an extra constraint to the problem. We measure time from the moment when the central density becomes infinite and define:

$$r_0 = -ct$$

$$\rho_0 = \frac{1}{4\pi G t^2}$$

and $$v_0 = c = \sqrt{\frac{\mathcal{R}T}{\mu}}: \text{ the isothermal sound speed.}$$

Then substituting into equations (11) to find a similarity solution, we find:

$$\left.\begin{aligned} (x+V)V' &= -\frac{N}{x^2} - Q' \\ 2+(x+V)Q' &= -V' - \frac{2V}{x} \end{aligned}\right\} \qquad (11)$$

and $$N' = x^2 \exp Q$$

where dashes denote differentiation with respect to x. We have in addition the boundary conditions:

$$V = Q' = 0 \text{ at } x = 0$$

and it would seem that we have an infinity of solutions according to how we pick $Q(0) = q$. However rewrite equations (11) as:

$$Q' + (x+V)V' = -\frac{N}{x^2}$$

$$(x+V)Q' + \qquad V' = -\frac{2(V+x)}{x}$$

and we find that when $x+V = \pm 1$ we have two prescriptions for $Q' \pm V'$. Accordingly we set

$$U = V + x$$

and solve equations (11) for Q' and V', i.e.

$$\left.\begin{aligned}(1-U^2)Q' &= -\frac{N}{x^2}+\frac{2U^2}{x}\\ (1-U^2)V' &= +\frac{NU}{x^2}-\frac{2U}{x}\\ N' &= x^2 \exp Q\end{aligned}\right\} \tag{12}$$

where we find that the solution will have a singularity where $U = \pm 1$ unless $N = 2x$ at that point also. This behaviour is the same as that of solar wind and other hydrodynamical solutions—there is a critical point in the flow. In order to obtain a smooth variation of density and velocity at this critical point, we must satisfy these further conditions there. To find the solution we must solve an eigenvalue problem, varying q until we find a solution where $U = 1$ and $N = 2x$ simultaneously. We show later that all solutions must have $U = 1$ at some point. Writing these conditions in dimensional form, we find our critical point where

$$r_{\text{crit}} = (c-v)(-t) = \frac{1}{2}\frac{GM_r}{c^2}.$$

Since the velocity at the critical point is constant r_{crit} is the distance from which sound waves can propagate to the centre before infinite density arises there. We see that at this point the gravitational energy per unit mass must be four times the thermal energy. The first criterion seems to imply that the flow must have some 'foreknowledge' of events which possibly means it is unstable. On the other hand the generality of the free-fall solution argues against this. We see that disturbances inside the critical point can propagate to the centre before the singularity occurs while this is not so outside the critical point. No stability analysis is attempted in this paper but this remains an important problem for the future.

Numerical integrations of equations (12) have revealed the eigenvalue $q = 0{\cdot}511$ and the accompanying runs of density and velocity, together with projected surface density, displayed in Fig. 3 and listed in Table II for some values of r/r_0.

We are interested in the form this solution takes at time $t = 0$, i.e. when the central density becomes infinite. To this end we investigate the form of the solution of equations (11) in the limit $x \gg 1$. If $V = o(x)$ as $x \to \infty$ we find:

$$-x^2Q' = -\frac{N}{x^2}+2x$$

$$-x^2V' = \frac{N}{x}-2$$

$$N' = x^2 \exp Q$$

which can be shown to possess the solution:

$$Q = Q_\infty+\ln\frac{2}{x^2}, \qquad N = 2x \exp Q_\infty, \qquad V = V_\infty+2\,\frac{\exp Q_\infty-1}{x} \tag{13}$$

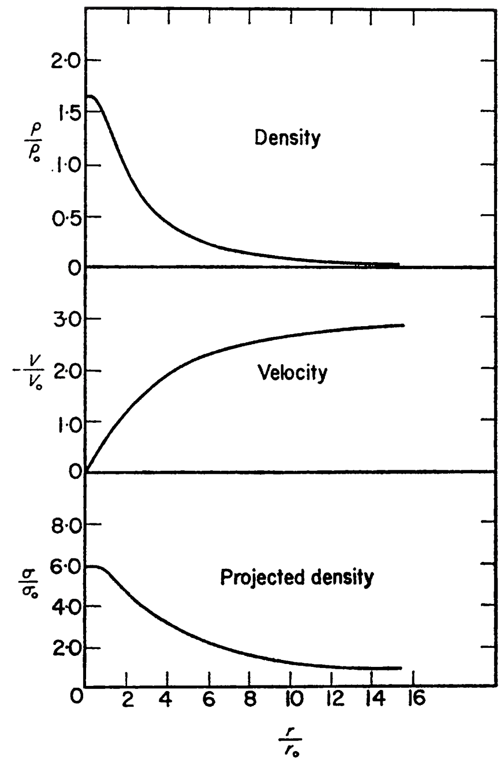

FIG. 3. *As fig. 2 but for the isothermal case. The profiles are the solution of equations* (11) *and are tabulated in Table II.*

TABLE II

Runs of density, velocity and projected surface density in the spherical isothermal similarity solution (see also Fig. 3)

r/r_0	ρ/ρ_0	$-v/v_0$	σ/σ_0 ($\sigma_0 = 2\rho_0 r_0$)
0·0	1·67	0·00	6·16
0·5	1·60	0·33	6·02
1·0	1·43	0·65	5·67
1·5	1·21	0·93	5·19
2·0	0·99	1·19	4·68
2·5	0·80	1·41	4·20
3·0	0·64	1·59	3·77
3·5	0·52	1·75	3·39
4·0	0·43	1·89	3·07
4·5	0·36	2·01	2·80
5·0	0·30	2·11	2·56
6·0	0·22	2·27	2·19
7·0	0·17	2·39	1·90
8·0	0·13	2·49	1·68
9·0	0·11	2·57	1·50
10·0	0·09	2·63	1·34
11·0	0·07	2·69	1·22
12·0	0·06	2·73	1·12
13·0	0·05	2·77	1·04
14·0	0·04	2·81	0·97
15·0	0·04	2·84	0·90

where V_∞ and Q_∞ are constants. Note that $V = o(x)$ as required, and that this is just the condition that $U \to x$ as $x \to \infty$. In addition $U = 0$ at $x = 0$ so that plainly $U = 1$ for some value of x between 0 and ∞. In other words the flow must possess a critical point.

Inspection of the full solution of equations (12) confirms that the similarity solution does indeed have the form of equations (13) as $x \to \infty$ with

$$Q_\infty \simeq 2\cdot 1 \simeq \ln 8\cdot 8 \text{ and } V_\infty \simeq -3\cdot 3.$$

Furthermore both show the behaviour $\rho \propto r^{-2}$ as found in the numerical computations of Bodenheimer & Sweigert (1968) and of Paper II. In full the dimensional form of the density and velocity profiles when the centre attains infinite density are:

$$\rho = 8\cdot 8 \frac{c^2}{4\pi G}\frac{1}{r^2}, \qquad v = -3\cdot 3c.$$

Here it is interesting to note that the density profile has the same r-dependence as that of the singular solution to the static isothermal gas sphere, however in this case the sphere suffers a constant supersonic inward velocity.

There are two further properties of this solution that are of interest. Firstly we may compute the Jeans number of this final solution as:

$$J = \frac{\dfrac{GM_r}{r}}{\dfrac{\mathscr{R}T}{\mu}} = \frac{N}{x} = 4\cdot 34$$

and note that the ratio of gravitational to thermal forces is also of order unity. This is a further illustration of the way the development of a density gradient by runaway evolution of a dense region can affect the dynamics, since in a uniform isothermal model one would expect the Jeans number of decrease as the collapse proceded. This ratio of gravitational to pressure forces is not so low that the Lynden-Bell–Mestel flattening instability (Lynden-Bell 1964; Mestel 1965) is totally suppressed. However this ratio must make the sphere more stable than in the free-fall case so that very likely the collapse proceeds in a similar way with a slightly ellipsoidal configuration. We show in Appendix I how in the free-fall case pressure forces become important due to the rise in density gradient earlier in planar collapses than in the spherical case.

Now we consider the optical depth of our collapsing sphere assuming a single-particle opacity due for example to dust or electron-scattering. Since $\sigma/\sigma_0 \simeq 6$ at the centre of the sphere, we can write the central optical depth as:

$$\tau \simeq 12\kappa\rho_0 r_0 = \frac{12\kappa c}{4\pi G}(-t)^{-1}$$

or, substituting for t, as

$$= 6\kappa c\left(\frac{\rho_0}{\pi G}\right)^{1/2}$$

a result which depends only on the density and temperature in the centre of the sphere. We can now find the central density at which a proto-star will go optically thick. Adopting $T = 10\,^\circ\mathrm{K}$, $\mu = 2$ and $\kappa = 4$ as observed in the Bok globules in the Orion Nebula (Penston 1969b) we find that $\tau = 1$ when:

$$\rho_{\text{central}} \simeq 1\cdot 7\rho_0 \simeq 10^{-18}\text{ g cm}^{-3}.$$

In this chapter we have found a similarity solution for a collapsing isothermal sphere with the similarity property found in Section 3 for the free-fall case. Its generality however remains in doubt since we have not yet shown that all isothermal collapses tend to this particular solution. To do so would involve a stability analysis which we have not attempted here, but it is encouraging that this solution reproduces the density law found by numerical work and this lends credence to its authenticity.

6. CONCLUSIONS

In Appendices I and II we give free-fall solutions for planar and cylindrical symmetries respectively analogous to the spherical solution of Sections 2–3.

The feature of these similarity solutions which makes them particularly important is their general accord with numerical solutions. They display the runaway of the densest regions so characteristic of these results and reproduce the density profiles found in the numerical work. Moreover in the free-fall case these solutions follow from quite general initial conditions and have simple parametric forms. On the other hand, the generality of the isothermal results is not yet established and a stability analysis of the isothermal solution is an important future project.

The solutions presented here show that star and galaxy formation proceed in a very non-homologous manner. A nucleus develops onto which the rest of the material subsequently falls, so that the later stages of formation take the form of accretion of the surrounding matter. It is tempting to identify the nuclei of galaxies with the density-peak formed in the collapse phases of their formation, however it seems more than probable that later events influence its detailed structure. However, the continuing infall of material at supersonic velocities onto the nucleus suggests that violent events should happen in galactic nuclei during their early stages so that it is by no means inconceivable that this process should give rise to the quasar phenomenon. Lynden-Bell (1967) has already remarked that there is sufficient energy released in galaxy-formation to account for the luminosity of quasars and here we have shown that the length scales involved are sufficiently small to explain their compactness as judged from radio observations.

On the other hand, we have shown that the optically thin stages of star-formation end when the proto-star is still very diffuse by the standards of stellar densities. Nonetheless our isothermal similarity solution ought to be useful as initial conditions for the optically thick stages of star formation, while the free-fall similarity solution will likewise give useful initial conditions for the later stages of star formation.

Finally the simple forms of our solutions should make them handy tools for investigating the effects of fragmentation and flattening instabilities in more realistic cases than the uniform collapses hitherto examined.

ACKNOWLEDGMENTS

It is a pleasure to acknowledge that the $r^{-12/7}$ law for the density profile of a freely-fallen sphere was first obtained by Miss Susan Storer (now Mrs Stobbs) and Dr D. Lynden-Bell. In addition it is acknowledged that the isothermal similarity solution described in Section 5 has been found independently by Dr R. B. Larson (1968).

The author is grateful to Dr D. Lynden-Bell both for stimulating discussions and a necessarily devastating criticism of an early draft of this work and to Dr B. Pagel for a critical reading of the final manuscript. The diagrams were drawn by Miss Rosemary Brett. All the computing in this paper was performed on the ICT 1909 in the Nautical Almanac Office at Herstmonceux.

Royal Greenwich Observatory, Herstmonceux Castle, Hailsham, Sussex.

Received in original form 1968 *December* 13.

REFERENCES

Abramowitz, M. & Stegun, I. A., 1964. *Handbook of Mathematical Functions*, U.S. Government Printing Office, Washington.
Bodenheimer, P. & Sweigert, A., 1968. *Astrophys. J.*, **152**, 515.
Disney, M. J., McNally, D. & Wright, A. E., 1968. *Mon. Not. R. astr. Soc.*, **140**, 319.
Larson, R. B., 1968. Unpublished Ph.D. Thesis, California Institute of Technology.
Lynden-Bell, D., 1964. *Astrophys. J.*, **139**, 1195.
Lynden-Bell, D., 1967. *I.A.U. Symposium No.* 31, p. 257.
McVittie, G. C., 1956. *Astr. J.*, **61**, 451.
Mestel, L., 1965. *Q. Jl R. astr. Soc.*, **6**, 161.
Penston, M. V., 1966. *R. Obs. Bull.*, No. 117.
Penston, M. V., 1969a. *Mon. Not. R. astr. Soc.*, (in press).
Penston, M. V., 1969b. *Mon. Not. R. astr. Soc.*, **144**, 159.

APPENDIX I

Free-fall in planar symmetry

In the main body of this paper, in Section 4, we have noted the potential importance of collapses in planar symmetry. It seems that any slight initial deviation from strict sphericity due to rotation, magnetism or any flattening will, assuming free-fall, evolved towards a flat configuration.

We consider a cold slab of gas initially at rest and with density $\rho(a)$ at distance a from the plane of symmetry. Then if $\bar{\rho}(a)$ is the mean density and $m(a)$ the mass within distance a of this plane:

$$m(a) = 2a\bar{\rho}(a) = \int_{-a}^{+a} \rho(x)\,dx.$$

The equation of motion is

$$\frac{d^2z}{dt^2} = \frac{dv}{dt} = -2\pi G m(a)$$

where z and v are the distance from the plane of symmetry and velocity of the material initially at a at time t. This has the solution:

$$z = a - \pi G m(a) t^2, \qquad v = -2\pi G M(a) t.$$

For a small, $z \to 0$ at time:

$$t = t_f = (2\pi G \rho_0)^{-1/2}$$

where

$$\rho_0 = \bar{\rho}(0) = \rho(0).$$

Following Sections 2–3 we assume $\bar{\rho}(a)$ is a maximum at $a = 0$—transferring our attention to a plane where it is a maximum if necessary—we may write.

$$\bar{\rho}(a) = \rho_0\left(1-\frac{a^2}{A^2}\right)$$

or

$$\rho(a) = \rho_0\left(1-3\,\frac{a^2}{A^2}\right).$$

We adopt two points of view, firstly we regard the above as complete exact initial conditions and then we take this density profile as an approximation valid for small a.

We find the full solution at time $t = t_f - \delta t = t_f(1-\tau)$. We have:

$$z = \frac{a^3}{A^2}(1-\tau)^2 + a\tau(2-\tau)$$

or using

$$\rho = \rho(a)\,\frac{da}{dz}$$

$$= \rho'_c\,\frac{1-3\beta\tau}{3\beta(1-\tau)^2(2-\tau)^{-1}+1} \qquad \text{(AI.1)}$$

where

$$\beta = \frac{a^2}{A^2}\left(\frac{\delta t}{t_f}\right)^{-1}$$

and

$$\rho'_c = \frac{\rho_0}{\left(2-\dfrac{\delta t}{t_f}\right)\dfrac{\delta t}{t_f}}.$$

We also have

$$\frac{z}{z_0} = \beta^{1/2}\{\beta(1-\tau)^2+(2-\tau)\} \qquad \text{(AI.2)}$$

where

$$z_0 = A\left(\frac{\delta t}{t_f}\right)^{3/2}.$$

Equations (AI.1) and (AI.2) are parametric equations relating ρ and z at time $t = t_f(1-\tau)$. We may include an equation for the velocity profile i.e.

$$\frac{v}{v_0} = -\beta^{1/2}(1-3\beta\tau)(1-\tau) \qquad \text{(AI.3)}$$

where

$$v_0 = \frac{2A}{t_f}\left(\frac{\delta t}{t_f}\right)^{1/2}.$$

Now these three numbered equations define the full solution of a collapse with planar symmetry having exactly the initial density distribution given above and are valid at any time. However we now take the other view that our density distribution is only the first terms of a series expansion and are only valid for a small. Then we can only obtain the runs of density and velocity near the plane of symmetry when $\tau \ll 1$ (i.e. at short times before the singularity arises on the plane of symmetry). We take the limit $\tau \to 0$ and find

$$\left.\begin{aligned} \frac{\rho}{\rho_c} &= \frac{1}{\frac{3}{2}\beta+1} \\ \frac{z}{z_0} &= \beta^{1/2}\{\beta+2\} \\ \frac{v}{v_0} &= -\beta^{1/2} \end{aligned}\right\} \qquad \text{(AI.4)}$$

where z_0 and v_0 are defined above and

$$\rho_c = \frac{1}{2}\rho_0\left(\frac{\delta t}{t_f}\right)^{-1}.$$

We recognize these as a similarity solution like that of Section 3, since all the time dependence now occurs in the scales ρ_c, v_0 and z_0. This similarity solution is displayed in Fig. 4 where the runs of density and velocity from equations (AI.4) are given.

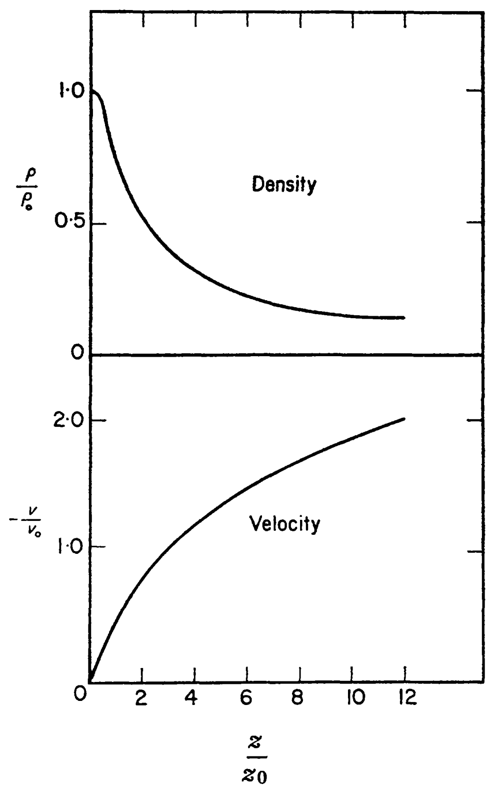

FIG. 4. *The planar free-fall similarity solution discussed in Appendix I. The profiles of density and velocity are plotted against distance from the plane of symmetry.*

To obtain the final forms of the density and velocity profiles as the density becomes infinite on the plane of symmetry we take the limit $z \gg z_0$ and find:

$$\frac{\rho}{\rho_c} = \frac{2}{3}\left(\frac{z}{z_0}\right)^{-2/3}, \qquad \frac{v}{v_0} = -\left(\frac{z}{z_0}\right)^{1/3}.$$

As in Section 3 these are independent of time and depend only on the initial conditions.

We now turn to the question of when and how planar collapses are halted. First of all note that the optical depth does not change as the collapse proceeds with this symmetry since it is proportional to $m(\infty)-m(a)$. Thus we only have to consider the thermal forces produced by the growth of the density gradient. We find the minimum in the ratio of gravitational to thermal forces is at the plane of symmetry and there:

$$J^* = -\frac{2GM(a)}{\frac{1}{\rho}\frac{d}{dz}\frac{\mathscr{R}T}{\mu}\rho} = \frac{16}{3}\frac{G\rho_c A^2}{\mathscr{R}T/\mu}\left(\frac{\delta t}{t_f}\right)^2$$

or using the same notation as Section 3 and making similar assumptions:

$$J^* = 4\frac{T_i}{T_f}\left(\frac{\delta t}{t_f}\right)^2.$$

Now we find that thermal forces become important much earlier than for spherical collapse when

$$\frac{\delta t}{t_f} \sim 10^{-1}$$

and at a density $\rho_c \sim \frac{1}{2}\, 10^{-29}\ \mathrm{g\ cm^{-3}}$, much lower than in the case of spherical symmetry.

Thus collapses in planar symmetry are opposed by thermal forces a lot sooner than spherical ones. We conclude that the Lynden-Bell–Mestel instability which may be the agent bringing about the deviations from spherical symmetry will be opposed, but not completely overcome, at an early stage by a rise in the pressure gradient.

APPENDIX II

Free-fall with cylindrical symmetry

For completeness we now derive the final velocity and density laws for the cylindrically symmetric case. This turns out to be more complex than either the spherical case or that with planar symmetry and since the cylindrical case is probably not very representative of nature we shall go no further.

Consider a cold cylinder of gas initially at rest and with density $\rho(a)$ at distance a from the axis. We define $\bar{\rho}(a)$ as the mean density and $m(a)$ the mass per unit length within radius a.
i.e.

$$m(a) = \pi a^2 \bar{\rho}(a) = \int_0^a 2\pi x \rho(x)\, dx.$$

Now the equation of motion is:

$$\frac{d^2r}{dt^2} = \frac{dv}{dt} = -\frac{2Gm(a)}{r}$$

where r and v are the distance from the axis and velocity at time t of material originally at a. Its solution is:

$$r = a\, e^{-\theta^2}$$

$$t = \frac{1}{\sqrt{(4G\bar{\rho}(a))}} \operatorname{erf} \theta$$

where θ is a parameter. We see that $r \to 0$ for small a when:

$$t = t_f = (4G\rho_0)^{-1/2}$$

where

$$\rho_0 = \bar{\rho}(0) = \rho(0)$$

Following the method of Section 2 we assume $\bar{\rho}(a)$ is a maximum at $a = 0$ and write:

$$\bar{\rho}(a) = \rho_0\left(1 - \frac{a^2}{A^2}\right)$$

and find the value of $\theta(a)$ at $t = t_f$. We have

$$1 = \left(1 + \frac{1}{2}\frac{A^2}{A^2}\right) \operatorname{erf} \theta(a).$$

To proceed we require an asymptotic expansion for erf θ for large θ. Abramowitz & Stegun (1964) give:

$$\sqrt{\pi}\, \theta\, e^{\theta^2} \operatorname{erfc} \theta \sim \sum_{m=0}^{\infty} (-1)^m \frac{1 \cdot 3 \ldots (2m-1)}{(2\theta^2)^m}$$

where

$$\operatorname{erfc} \theta = 1 - \operatorname{erf} \theta.$$

This series diverges since the terms do not satisfy the ratio test. However $R_n(\theta)$, the remainder after n terms, is less in absolute value than the first neglected term and of the same sign. So for $\theta \gg 1$ we may write:

$$\operatorname{erf} \theta \sim 1 - \frac{e^{-\theta^2}}{\sqrt{(\pi)}\theta}$$

Using this for a small (and hence θ large):

$$a^2 = \frac{2A^2}{\sqrt{\pi}} \frac{e^{-\theta^2}}{\theta}$$

and

$$r^2 = \frac{2A^2}{\sqrt{\pi}} \frac{e^{-3\theta^2}}{\theta}. \qquad \text{(AII.1)}$$

Further using

$$\rho \simeq \rho_0 \frac{da^2}{dr^2}$$

we obtain

$$\rho = \tfrac{1}{3} \rho_0 e^{2\theta^2}. \qquad \text{(AII.2)}$$

We cannot eliminate θ to obtain density in terms of radius at time $t = t_f$ but the profile is nonetheless described parametrically by equations (AII.1) and (AII.2). As $r \to 0$, the density exceeds $Ar^{-4/3}$ for any positive A but is exceeded by $Ar^{-4/3-\epsilon}$ for any positive ϵ however small.

We can also obtain the velocity run at time $t = t_f$ in parametric form as

$$v^2 = 4\pi G\rho_0 \left(\frac{3A^2}{\sqrt{\pi}}\, \theta e^{-\theta^2}\right) \qquad \text{(AII.3)}$$

together with equation (AII.1). Again we may say that the modulus of the velocity exceeds $Ar^{1/3}$ as $r \to 0$ for any positive A but is exceeded by $Ar^{1/3-\epsilon}$ for any positive ϵ however small.